Supporting Online Material for

Axle-Less F_1-ATPase Rotates in the Correct Direction

Shou Furuike, Mohammad Delawar Hossain, Yasushi Maki, Kengo Adachi, Toshiharu Suzuki, Ayako Kohori, Hiroyasu Itoh, Masasuke Yoshida, Kazuhiko Kinosita Jr.*

*To whom correspondence should be addressed. E-mail: kazuhiko@waseda.jp

Published 15 February 2008, *Science* **319**, 955 (2008)
DOI: 10.1126/science.1151343

This PDF file includes:

Other Supporting Online Material for this manuscript includes the following:
(available at www.sciencemag.org/cgi/content/full/319/5865/955/DC1)

Supporting Online Material

Online Movie 1
Rotation of a 40-nm gold bead attached to γ-ΔN22C43 (2 mM ATP).
This movie corresponds to N22C43 in Fig. 3D, -1 s to 15 s. Blue frames indicate irregular motions, and green frames backward steps. Original images (390×390 nm^2 = 7×7 pixels) have been Gaussian-filtered and 8× magnified to aid perceive rotation. Original movie at 125 frames s^{-1} is replayed at 25 frames s^{-1} (5× slow replay).

Online Movie 2
Rotation of a 40-nm gold bead attached to γ-ΔN18C40 (2 mM ATP).
This movie corresponds to N18C40 in Fig. 3D, 0 s to 8 s. Blue frames indicate irregular motions, and green frames backward steps. Original images (390×390 nm^2 = 7×7 pixels) have been Gaussian-filtered and 8× magnified. Original movie at 250 frames s^{-1} have been re-sampled at 125 frames s^{-1} and is replayed at 25 frames s^{-1} (5× slow replay).

Online Movie 3
Rotation of a 40-nm gold bead attached to γ-ΔN14C36 (2 mM ATP).
This movie corresponds to lower N14C36 in Fig. 3A, 17 s to 22 s. Blue frames indicate irregular motions. Original images (390×390 nm^2 = 7×7 pixels) have been Gaussian-filtered and 8× magnified. Original movie at 500 frames s^{-1} have been re-sampled at 125 frames s^{-1} and is replayed at 25 frames s^{-1} (5× slow replay).

Online Movie 4
Rotation of a 40-nm gold bead attached to wild-type TF_1 (2 μM ATP).
This movie corresponds to wild type in Fig. 3C, 0 s to 1 s. Original images (390×390 nm^2 = 7×7 pixels) have been Gaussian-filtered and 8× magnified. Original movie at 8,000 frames s^{-1} have been re-sampled at 1,000 frames s^{-1} and is replayed at 25 frames s^{-1} (40× slow replay).

Online Movie 5

Rotation of a 0.29-μm polystyrene bead duplex attached to γ-ΔN7C29 (2 mM ATP).

This movie corresponds to the lowest N7C29 in Fig. 4A, 0 s to 40 s. Original movie at 500 frames s^{-1} have been re-sampled at 25 frames s^{-1} (real time replay).

Online Movie 6

Rotation of a 0.29-μm polystyrene bead duplex attached to wild type TF_1 (200 nM ATP).

This movie corresponds to wild type in Fig. 4A, 0 s to 40 s. Original movie at 500 frames s^{-1} have been re-sampled at 25 frames s^{-1} (real time replay).

Materials and Methods

Molecular genetics and confirmation of truncation

Mutations were made on plasmid pKABG1/HC95 that carries genes for the α (C193S), β (His_{10} at amino terminus), and γ (S107C, I210C) subunits of TF_1 (*S1*, *S2*). We introduced γ C-terminal truncations in pKABG1/HC95 as previously described (*S3*). First, we transferred a *Bgl*II-*Mlu*I fragment of plasmid pKABG1/HC95 containing the region coding γ (thick arrow in the diagram) into a plasmid derivative of pET-42b(+) (Novagen, Tokyo) in which *Xho*I-*Eco*RI region had been replaced with a fragment lacking an *Hind*III site. The resultant plasmid contained a sole *Hind*III-*Nhe*I region, which encompassed the γ C-terminus. To mutate this region, we prepared an *Hind*III-*Nhe*I fragment with a desired γ truncation by PCR amplification using pKABG1/HC95 as template and the following primers.

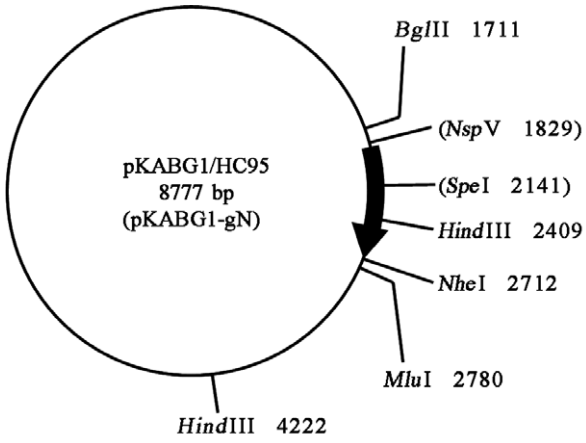

A forward primer containing an *Hind*III-site:

5′-GGAAGCTTCTGCCGCTCACTGAC-3′

Reverse primers containing an *Nhe*I-site:

for γ-ΔC25,

5′-GGGCTAGCTTATTAAAGCGTCAATGTGCGAATGAGCTCG-3′

for γ-ΔC29, 5′-GGGCTAGCTTATTAGCGAATGAGCTCGTTCGCATTG-3′

for γ-ΔC32, 5′-GGGCTAGCTTATTACTCGTTCGCATTGTCCGTTGC-3′

for γ-ΔC36, 5′-GGGCTAGCTTATTAGTCCGTTGCGTTCTTCATCGC-3′

for γ-ΔC40, 5′-GGGCTAGCTTATTACTTCATCGCCGTCATCCGG-3′

for γ-ΔC43, 5′-GGGCTAGCTTATTACGTCATCCGGGCGGCGTGTT-3′

The *Hind*III-*Nhe*I portion of the amplified fragment was transferred back to the modified pET-42b(+), and its *Bgl*II-*Mlu*I fragment was introduced into pKABG1/HC95 to produce the expression plasmid pKABG1/HC95(γ-ΔC).

For N-terminal truncations, we first introduced into pKABG1/HC95 an *Nsp*V site immediately upstream the γ-coding region and an *Spe*I site ~300 bases down stream by silent mutations using QuickChange XL Site-Directed Mutagenesis kit (Stratagene, CA). We refer to this plasmid as pKABG1-gN. Primers used for the *Nsp*V site were

5′-CGCCTGTTAGAACCCGTGTTCGAAAAAGGAGGTGAAACCCATGGC-3′

and

5′-GCCATGGGTTTCACCTCCTTTTTCGAACACGGGTTCTAACAGGCG-3′,

and those for the *Spe*I site were

5′-GCAACGTGTTGCGACTAGTGTACCAAACGATCCAAAAACG-3′

and

5′-CGTTTTTGGATCGTTTGGTACACTAGTCGCAACACGTTGC-3′

where underscores show mutations.

We then introduced the γ-ΔC mutations into pKABG1-gN by replacing its *Spe*I-*Mlu*I portion with a truncated sequence. The latter was obtained by PCR using pKABG/HC95(γ-ΔC) above as template and a forward primer containing an *Spe*I site

5′-GCAACGTGTTGCGACTAGTGTACC-3′

and a reverse primer containing an *Mlu*I site

5′-CTTGGATAACGCGTCCTCTTGTC-3′.

Finally, we introduced N-terminal truncations by replacing the *Nsp*V-*Spe*I portion that encompasses the γ N-terminus with a truncated sequence. The truncated sequences were obtained by PCR using pKABG1-gN as template and following primers.

A reverse primer containing an *Spe*I-site:

5′-GGTACACTAGTCGCAACACGTTGC-3′

Forward primers containing an *Nsp*V site:

for γ-ΔN4C25, 5′-GAACCCGTGTTCGAAAAAGGAGGTGAAACCCATGGATA-TTAAAACGCGC-3′

for γ-ΔN7C29, 5′-GAACCCGTGTTCGAAAAAGGAGGTGAAACCCATGACGC-GCATCAATGCG-3′

for γ-ΔN11C32, 5′-GAACCCGTGTTCGAAAAAGGAGGTGAAACCCATGGCG- ACGAAGAAGACAAGCC-3′

for γ-ΔN14C36, 5′-GAACCCGTGTTCGAAAAAGGAGGTGAAACCCATGAAG-ACAAGCCAAATTACAAAAGCG -3′

for γ-ΔN18C40, 5′-GAACCCGTGTTCGAAAAAGGAGGTGAAACCCATGATT-ACAAAAGCGATGG-3′

for γ-ΔN22C43, 5′-GAACCCGTGTTCGAAAAAGGAGGTGAAACCCATGATG-GAAATGGTCTCG-3′.

The mutant lacking γ entirely, the $\alpha_3\beta_3$ complex, was produced by introducing into pKABG1-gN two *Xho*I sites, one between *Nsp*V site and the beginning of the γ coding region and the other between the end and *Nhe*I site, and then removing the *Xho*I-*Xho*I portion. The replacement sequence was obtained by PCR using pKABG1-gN as template and a reverse primer containing an *Nhe*I and an *Xho*I sites

5′- AAATTTGCTAGCCTCGAGCTCGTTCGCATTGTCCGTTGC-3′

and a forward primer containing an *Nsp*V and an *Xho*I sites

5′-GAACCCGTGTTCGAAAAAGCTCGAGGTGAAACCC-3′

where underscores show mutations.

All mutations above were confirmed by DNA sequencing (FASMAC Co., Ltd., DNA sequencing services, Atsugi, Japan). In *E. coli* strain JM103 Δ(uncB-uncD) which has lost the ability to express authentic F_oF_1-ATPase (*S4*), all mutants were expressed to a level similar to wild type, as seen in fig. S1. The N-terminal five residues of expressed γ were confirmed by Edman degradation (APRO Life Science Institute, Inc., Naruto, Japan) as shown in table S1. The initiation residue Met-1 was absent in the wild type, γ-ΔN7C29 (~30% had Met-1), and γ-ΔN11C32. The mutants γ-ΔN4C25, γ-ΔN7C29, γ-ΔN11C32, and γ-ΔN14C36 were also checked by MALDI-TOF mass spectrometry (APRO Life Science

Institute) as shown in table S1. Peaks corresponding to α, β, and γ subunits were obvious except for γ-ΔN14C36, for which the γ peak appeared on a side of the β (z=2) peak.

[The amino-acid sequence here and in Fig. 1B in the main text is from ref. *S5*, except that our numbering in this work and in ref. *S3* starts from Met-1, which is absent in the expressed wild type. Recently we have found that the actual sequence of TF_1 that we used here (and in ref. *S3*) is slightly different from the original one in ref. *S5* and that the C-terminus of the wild type in this work is Gln-285 and not Gln-283, counting from Met-1 (T. Suzuki and M. Yoshida, unpublished). Because the differences are not in the N- and C-termini, we adopt the published sequence for description of truncation. The expected masses in the table below, however, have been calculated on the basis of the actual sequence.]

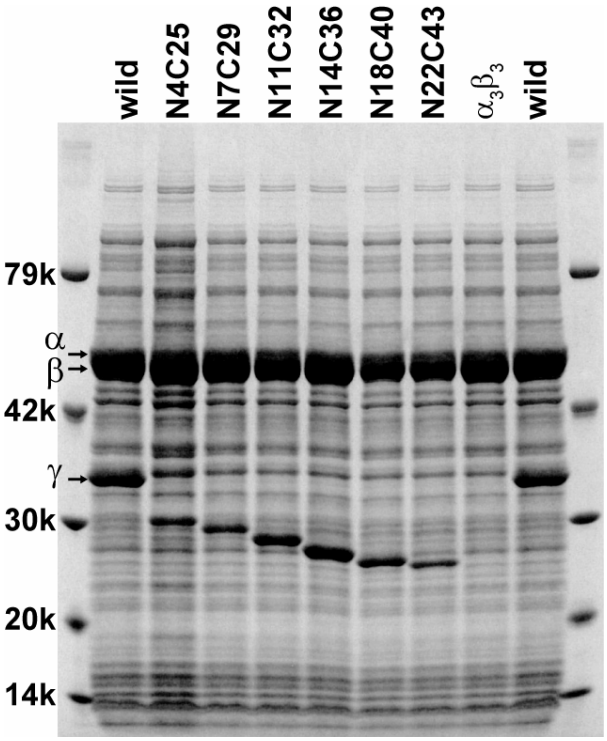

fig. S1. Expression of αβγ subunits of TF_1 in *E. coli*. *E. coli* pellets were dissolved in 2% SDS and, after centrifugation to remove insoluble materials, applied to 12.5% polyacrylamide gel containing 0.1% SDS. Stained with Coomassie Brilliant Blue R-250.

table S1. Confirmation of γ truncations

Mutant	Amino acid sequence at N-terminus of γ (right to left)*	Experimental mass *m/z* (*z* = 1)			Expected mass of γ	
		α	β	γ	*m/z*	sequence
Wild type	-DRLSA	54714.8 (expected)	53355.9 (expected)			
γ-Δ**N4C25**	-TKID*M*	54720	53360	28720	28728.2	Met5-Leu258
γ-Δ**N7C29**	-ANIRT (~70%) -NIRT*M* (~30%)	54720	53360	27800	27812.0	Thr9-Arg254
γ-Δ**N11C32**	-TKKTA	54720	53360	26940	26945.0	Ala13-Glu251
γ-Δ**N14C36**	-QSTK*M*	54720	53360	26350	26347.4	Met15-Arg247
γ-Δ**N18C40**	-AK(T)I*M* (T: unclear)					
γ-Δ**N22C43**	-VMEM*M*					

*Italic *M* indicates undigested Met-1.

Purification of F_1 and the measurement of ATP hydrolysis activity

Mutant TF_1's were expressed in *E. coli* strain JM103 Δ(uncB-uncD), purified and biotinylated as described (*S6*), except that heat treatment and passage through a butyl-Toyopearl column (for removal of bound nucleotide) were omitted. (Samples of wild type, γ-ΔC17, and γ-ΔC21 for hydrolysis assay were passed through a butyl column.) The passages through a Ni^{2+}-NTA superflow column (Qiagen, Hilden, Germany) and a size-exclusion column (Superdex 200, 10/300 GL, GE Healthcare UK Ltd., UK) and biotinylation were done and purified TF_1 was kept at room temperature. Mutant proteins were used immediately, within at most three days.

The rate of ATP hydrolysis by the mutants was measured at 10-20 nM F_1, without biotinylation, at 23°C by coupling the reaction with consumption of NADH (*S3*); the rate was estimated in the initial ~20 s period (fig. S2).

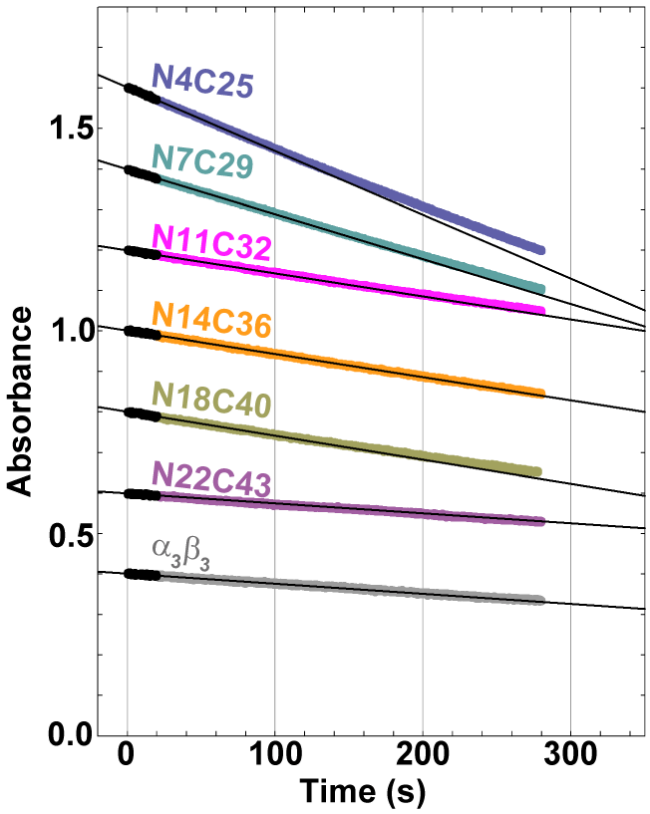

fig. S2. Time courses of ATP hydrolysis at 2 mM ATP by 10 nM mutant F_1. A decrease in absorbance by 0.622 corresponds to consumption of 100 μM ATP. Hydrolysis rates were estimated in the initial 20-s portion (thick black), as shown by the thin black lines. Temperature, 23°C.

Observation of rotation with gold beads

We modified the surface of 40-nm gold beads (EM.GC40, a suspension at 9×10^{10} particles ml^{-1}, BBInternational, Cardiff, UK) with polyethylene glycol (PEG) and PEG-biotin by adding 0.2 mM 2-aminoethanthiol (Tokyo Chemical Industry, Tokyo), 0.1 mM NHS-m-dPEG (molecular weight: 1214, Quanta BioDesign, Powell) and 0.1 mM NHS-dPEG4-Biotin (Quanta BioDesign) to the bead suspension and letting the reaction proceed at room temperature for more than one day. Before use, we washed the gold beads extensively with buffer A (10 mM Mops-KOH, pH 7.0, 50 mM KCl) to remove free biotin.

Biotinylated TF_1 (10-100 nM) in 10 mM Mops-KOH, 20 mM imidazole-HCl, pH7.0, 400 mM KCl, or in buffer A for wild type, γ-ΔC17, and γ-ΔC21, was infused into an observation chamber made of Ni-NTA coated bottom and uncoated top coverslips (*S3*). After washing out unbound TF_1 with buffer A, we infused 10 mg ml^{-1} BSA in buffer A to

prevent nonspecific binding, and then 40 μg ml^{-1} streptavidin (Pierce, Rockford) in buffer A. After extensive washing with buffer A, we infused the modified gold beads and washed away excess beads with buffer A. Finally, we infused buffer A containing 2 mM MgATP, 2 mM $MgCl_2$, and an ATP regenerating system (0.2 mg ml^{-1} creatine kinase and 2.5 mM creatine phosphate).

Bead rotation was observed at 23°C by laser dark-field microscopy (*S2*) with some modifications (S. Furuike, unpublished), on an inverted microscope (Olympus IX70). Images were captured with a high-speed CMOS camera (FASTCAM-DJV, Photron, Tokyo) at 125 to 8,000 frames s^{-1} as an 8-bit AVI file. Centroid of bead images was calculated as described (*S2*).

Observation of rotation with polystyrene beads

Biotinylated TF_1 (10-100 nM) was infused into an observation chamber made of Ni-NTA coated bottom and uncoated top coverslips (*S3*). Streptavidin-coated polystyrene beads of diameter 0.29 μm (Seradyn) were infused, followed by buffer A containing 2 mM MgATP, 2 mM $MgCl_2$ and the ATP regenerating system. Rotation was observed at 23°C on an inverted microscope (Olympus IX71) with a stable mechanical stage (KS-O, Chuukousha-Seisakujo, Japan). Ordinary transmission images of the beads were captured with a CCD camera (IPX-210M, Lynx) at 500 frames s^{-1} as an 8-bit AVI file. The apparent torque was estimated from the instantaneous speed during stepping rotation as described (*S3*).

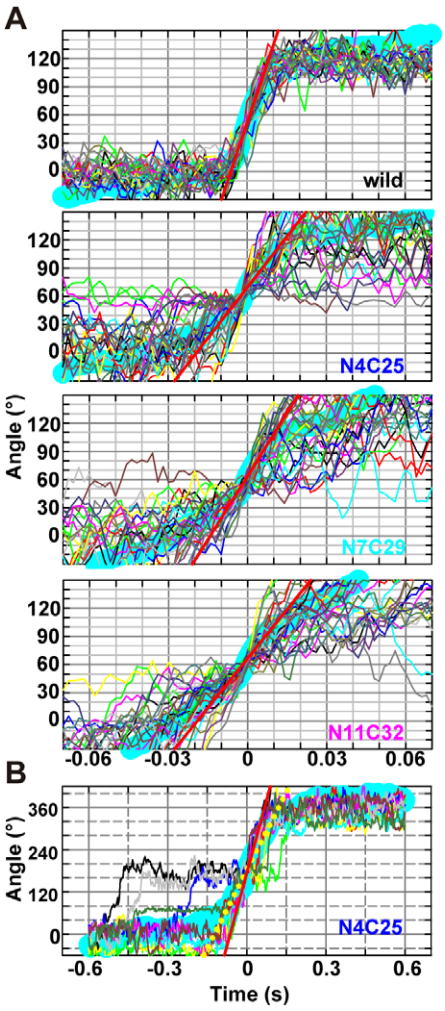

fig. S3. Estimation of torque from rotation of 0.29-μm bead duplexes. (**A**) Torque estimation from the instantaneous rotary speed during 120° steps. Thin colored lines show 30 consecutive steps, thick cyan lines being the average. Individual step records have been shifted vertically by a multiple of 120° to obtain the overlap. Time zero for each step record was assigned by eye to the data point closest to 60°. Straight red lines fit the cyan line between 30° and 90°. Torque was calculated as the slope of the red line (in radian s^{-1}) times the frictional drag coefficient of the bead duplex (0.28-0.34 pN·nm·s). Wild type gave torque values of 44±4 pN·nm (mean±SD, n = 3); γ-ΔN4C25, 23±3 pN·nm (n = 3); γ-ΔN7C29, 22±2 pN·nm (n = 3); γ-ΔN11C32, 18 pN·nm (n = 1). (**B**) Torque estimation from triplets of 120°-steps. Colored thin lines show 10 consecutive triplets in Fig. 4A, γ-ΔN4C25, arrow. Thick cyan line, average; red line, fit between 150° and 210°; yellow dotted line, fit between 60° and 300°. The yellow line gives a torque of 8.3 pN·nm, which should be an underestimate because some of the curves are stuck in the middle.

Supporting References

S1. T. Matsui, M. Yoshida, Expression of the wild-type and the Cys-/Trp-less $\alpha_3\beta_3\gamma$ complex of thermophilic F_1-ATPase in *Escherichia coli*, *Biochim. Biophys. Acta* **1231**, 139-146 (1995).

S2. R. Yasuda, H. Noji, M. Yoshida, K. Kinosita Jr, H. Itoh, Resolution of distinct rotational substeps by submillisecond kinetic analysis of F_1-ATPase, *Nature* **410**, 898-904 (2001).

S3. M. D. Hossain, S. Furuike, Y. Maki, K. Adachi, M. Y. Ali, M. Huq, H. Itoh, M. Yoshida, K. Kinosita Jr, The rotor tip inside a bearing of a thermophilic F_1-ATPase is dispensable for torque generation, *Biophys. J.* **90,** 4195-4203 (2006).

S4. R. A. Monticello, E. Angov, W. S. A. Brusilow, Effects of inducing expression of cloned genes for the F_o proton channel of the *Escherichia coli* F_1F_o ATPase, *J. Bacteriol.* **174**, 3370-3376 (1992).

S5. S. Ohta, M. Yohda, M. Ishizuka, H. Hirata, T. Hamamoto, Y. Otawara-Hamamoto, K. Matsuda, Y. Kagawa, Sequence and over-expression of subunits of adenosine triphosphate synthase in thermophilic bacterium PS3, *Biochim. Biophys. Acta* **933**, 141-155 (1988).

S6. K. Adachi, H. Noji, K. Kinosita Jr, Single-molecule imaging of rotation of F_1-ATPase, *Methods Enzymol.* **361B**, 211-227 (2003).